This is a repository copy of *Combined rupture mechanisms in shallow foundations*.

White Rose Research Online URL for this paper:
http://eprints.whiterose.ac.uk/123009/

Version: Accepted Version

Article:
Gajo, A. and Smith, C.C. orcid.org/0000-0002-0611-9227 (2018) Combined rupture mechanisms in shallow foundations. Canadian Geotechnical Journal. ISSN 0008-3674

https://doi.org/10.1139/cgj-2016-0324

Reuse
Items deposited in White Rose Research Online are protected by copyright, with all rights reserved unless indicated otherwise. They may be downloaded and/or printed for private study, or other acts as permitted by national copyright laws. The publisher or other rights holders may allow further reproduction and re-use of the full text version. This is indicated by the licence information on the White Rose Research Online record for the item.

Takedown
If you consider content in White Rose Research Online to be in breach of UK law, please notify us by emailing eprints@whiterose.ac.uk including the URL of the record and the reason for the withdrawal request.

eprints@whiterose.ac.uk
https://eprints.whiterose.ac.uk/

COMBINED RUPTURE MECHANISMS IN SHALLOW FOUNDATIONS

A. Gajo and C. C. Smith

Abstract

Conventional ultimate limit state (ULS) shallow foundation design is typically based on a simplified analysis that fails to consider the possible existence of a combined structural and geotechnical failure, which is shown here to significantly affect the limit load. Neglecting this occurrence may lead to unsafe design, whereas a full analysis can be beneficial for the dimensioning. With the emphasis on separate SLS and ULS design in modern design codes such as Eurocode 7 (EN 1997-1, 2004), this paper explores unsafe loading scenarios and the benefits to be gained from a rigorous ULS design based on combined failure. For the sake of simplicity, a long foundation slab subjected to three different loading conditions is analysed using elastic, elasto-plastic and rigid-plastic methods and the results compared for a range of foundation strengths and stiffnesses. It is found that the limit load may be significantly influenced by plastic hinges in the structure and for each load condition it is possible to derive a curve relating ultimate load to plastic bending moment representing the ultimate limit state of the foundation.

Introduction

The evaluation of the ultimate limit state (ULS) load capacity of shallow foundations is a standard and well-accepted procedure for foundations (such as isolated footings), which do not undergo any structural rupture themselves and in which the rupture mechanism develops only in the soil beneath the foundation. The situation can be completely different in deformable foundation structures (such as beams and slabs) in which, for applied loads well below the limit load of a fully rigid foundation, plastic hinges may form in the foundation structure leading to combined rupture mechanisms which develop partly in the soil and partly in the foundation structure itself. This case must be treated by considering a global mechanism of collapse. To the authors' knowledge, this possibility is not usually taken into account in current design practice of shallow foundation design (e.g. Fang, 1991, Smoltczyk, 2003, Burland et al. 2012) and has never been analysed from a theoretical point of view, notwithstanding the fact that in the current design practice the combined rupture in the soil and in the structural element is routinely taken into account for other geotechnical structures such as horizontally-loaded, flexible piles (see Broms' theory) or sheet pile walls (see Ukritchon et al., 2003, for braced excavations). In fact, although Eurocode EN 1997-1 differentiates between stiff and flexible foundations, it does not give any guidance on how to take account of soil-foundation interaction at ULS for the evaluation of the bearing pressure distribution under a flexible foundation (e.g. Frank et al. 2004).

Unfortunately, neither theoretical nor numerical instruments are available for this kind of analysis, nor experimental measurements have ever been performed. Therefore, the analyses that will be shown below are a first attempt to consider this problem and concern

the combined ruptures occurring in a very simple, plane strain case representing a very long foundation slab, resting on a thick layer of soft clay, loaded under undrained conditions. The results will be compared with conventional analysis. To gain full insight into the problem, the analysis is performed using four different methods:

1. Conventional methods where the pressure on the foundation base is derived from an analysis involving failure in the soil only.
2. Rigid-plastic analysis using the upper bound computational limit analysis (CLA) method Discontinuity Layout Optimization (DLO) (Smith and Gilbert, 2007),
3. Elasto-plastic finite element analysis (EPFEM) performed with both ABAQUS (Hibbitt, Karlsson & Sorensen, 2009) and PLAXIS (Brinkgreve, 2002)
4. A Winkler model using (i) linear elastic springs (LW) and (ii) linear elastic-perfectly-plastic springs (NLW), working only in compression in both cases; these models were analysed with ABAQUS (Hibbitt, Karlsson & Sorensen, 2009).

The specific objectives are:

1. compare the elasto-plastic, rigid-plastic, and the Winkler models (LW, NLW), to determine the relative abilities of each method to analyse the combined soil/structure ULS;
2. compare the ULS plastic moment of resistance derived from a combined soil and structural failure mechanism with typical serviceability limit state (SLS) bending moments.

The manuscript is not intended to be exhaustive in providing a complete and easily applicable method of analysis for current design practice. The aim of the work is rather to drive reader's attention to a new class of soil-foundation interaction at ULS that has never been considered so far and that will deserve much more attention in the future for its theoretical treatment and experimental validation. Future developments will certainly have to provide routine analysis methods for considering foundations beam and slabs, subjected to complex loading conditions, under undrained and drained conditions.

However the present work does not simply show the unexpected effects of a combined rupture mechanism, but it is also helpful for evaluating the cases of potentially unsafe design, that can be avoided by over dimensioning the structure if a full analysis is not performed. For simplicity, the presented analyses are limited to undrained conditions which is sufficient to illustrate the key concepts. Here the associative flow rule required by rigid-plastic limit analysis is normally taken as a good representation of undrained behaviour and requires no further consideration. In contrast drained analyses are much more complex to be performed from a numerical point of view, and would require consideration of the possible impact of non-associativity and the effects of foundation size on bearing capacity.

The SLS condition has been considered by assuming a simple linear elastic response, as an approximation to the actual non-linear stress-strain response of soil (see e.g. Vardenaga & Bolton, 2011). This allows indicative results to be obtained while retaining a simple, commonly used method in engineering practice.

The paper is organized as follows: the problems are firstly described and analysed through a conventional and a simplified analysis at ULS. Then the limit loads and the maximum bending moments are evaluated through different methods and are compared with each

other, leading to the definition of a limiting (or yield) surface (in a space of applied load versus maximum bending moment) for each loading condition. The discussion and the conclusions are finally given.

Problem definition of exemplar cases

The problem will be examined for an infinitely long shallow foundation of width B=10 m (i.e. plane strain) for the three configurations of load distribution A-C shown in Table 1.

The selected geometric condition and load distributions are intended to represent a broad range of practical situations, on which simple theoretical reasoning is possible. In particular the load distributions A and B can be considered representative of a beam foundation in which the most heavily loaded pillars are the central and the lateral ones, respectively. Load distribution C is representative of a condition with high eccentricity. It is assumed that the applied load is not influenced by settlements, thus the load conditions are typical of an overlying structure which is much more deformable than the foundation. Otherwise, the kinematic constraint of the overlying structure should be considered.

The subsoil is assumed uniform with an undrained shear strength of c_u=20 kPa for illustrative purposes. The foundation is perfectly shallow (i.e. the depth of the foundation base is zero) with the soil surface on either side under zero surcharge and the base of the foundation is assumed to be perfectly smooth. A no-tension interface was assumed between the soil and the foundation. Different values of the plastic moment of resistance M_p are assumed for the shallow footing, ranging between 100 and 1000 kNm/m.

The EPFEM analyses require the elastic behaviour to be considered, although, from plasticity theory, the elastic stiffness should be irrelevant at the ultimate limit state condition for an undrained problem. The subsoil stiffness was assumed as E_u=20 MPa (from the ratio E_u /c_u =1000 which is meaningful value for a soft clay, e.g. Duncan & Buchigani, 1976), whereas two values of beam stiffness were assumed corresponding to different height concrete sections, h = 31 cm and h = 90 cm, made with a concrete having f_{bk}=30 MPa (namely E=24.2 GPa and Poisson ratio 0.3), which gives beam stiffnesses of EJ=0.06x10^6 kNm^2/m and EJ=1.47x10^6 kNm^2/m respectively. The Poisson ratio of the subsoil was assumed to be 0.495 to ensure the volumetric incompressibility typical of undrained conditions, without inducing numerical difficulties.

Conventional ULS Analysis assuming a stiff foundation

At ULS, conventional analysis assumes a uniform pressure distribution beneath the base of the foundation. The calculations to determine the limit load and maximum bending moment using this assumption are therefore straightforward and are summarized in Table 1.

For the eccentrically load case C, the assumed ULS pressure distribution is assumed to be uniform and limited to an effective bearing width B' (Meyerhof, 1953). This simple pressure distribution will be shown to be consistent with maximum bending moments evaluated with numerical analyses.

For a non-yielding foundation, the limit loads calculated in Table 1 for non-eccentric loadings are known to be exact plastic solutions, while for eccentrically loaded foundations, Ukritchon et al (1998) have shown that for zero surcharge (q = 0), the collapse load calculated by the Meyerhof approach closely matches their numerical lower bound and upper bound solutions and can therefore also be assumed to be close to exact.

An assumption of uniform bearing pressure can therefore be used to determine a simple lower bound solution that includes both soil and foundation and is close to exact in terms of collapse load. This will enable definitive statements to be made concerning solutions to be derived later in the paper. For a lower bound, it is necessary to find a stress field in the soil that is a valid equilibrium stress field not violating yield and is in equilibrium with the uniform pressure $c_u N_c$ on the interface between the soil and foundation. This can be provided by the standard undrained footing lower bound solution. Additionally, assuming conventional beam bending theory is considered valid, the stress state in the foundation is also an equilibrium stress field not violating yield within the foundation, and also in

equilibrium with (i) the structural loading applied to the top of the foundation and (ii) the uniform pressure $c_u N_c$ along the pressure bearing interface between the soil and foundation. It is assumed that yield is not violated if the maximum bending moment does not exceed the bending strength. (Other yield violations e.g. in shear are possible but assumed unlikely).

Therefore if the bending strength is specified as the derived maximum moment based on a uniform pressure distribution and the equations of Table 1, then the result is a lower bound solution for the collapse load. It will always carry the load and may be able carry a higher load.

Further statements may be made using the following theorem of plasticity (Chen, 2007):

"*Increasing (decreasing) the yield strength of the material in any region cannot weaken (strengthen) the body.*" (Theorem 1)

Reduction of the foundation strength can therefore only lead to a lower or the same collapse load. Hence combined rupture will occur at a lower or equal load to those predicted above.

Simple Analysis of Bending Moments for loads below the ULS

At loadings lower than that required to generate a ULS in either soil or structure, the pressure distribution may be estimated as a uniform pressure in the same way as for the ULS, but scaled proportionally to the loading (in effect mobilising only part of the soil strength) allowing equations of Table 1 to be used. This will be termed a *scaled-ULS*

analysis. This approach is straightforward although it is only approximate, in particular when the distribution of contact pressures is evaluated with FEM for SLS conditions that more closely resemble an elastic stress field, for which a Boussinesq like pressure distribution would be expected.

For the common case of an undrained soil and horizontal soil surface the status of this scaled-ULS solution can be straightforwardly determined using the previously quoted theorem of plasticity.

Consider a foundation design for a soil of undrained strength c_u/n, where n is a scale factor. Eccentricity is unaffected by the change in bearing pressure and therefore the collapse load and maximum bending moments will be linear functions of the bearing pressure and are thus also scaled by the factor n. A foundation with bending strength scaled by n will always be able to carry a load also scaled by n.

Using Theorem 1, increasing the undrained soil strength back to c_u cannot weaken the body, therefore the scaled collapse load is also a lower bound to the scenario of a scaled foundation bending strength and the original soil strength. However it is likely to be a significant underestimate and a combined rupture analysis is recommended to ensure maximum utilisation of the soil and structural strengths.

Note that theorem 1 applies to the exact solution (namely when the upper and lower bounds coincide with each other) and works also with the lower bound when the soil is strengthened. As a result, the reasoning given above can be applied to symmetrically loaded foundations and for eccentrically loaded foundations (where $q = 0$).

Limit loads from DLO and EPFEM analyses

The DLO procedure directly determines the limit load using optimization techniques to identify the critical collapse mechanism. Since the foundation stiffness is not relevant in a CLA analysis, the footing was modelled as a one dimensional element with a specified plastic moment of resistance. The method discretises the domain into a grid of nodes and the critical collapse mechanism is constructed from a discrete set of slip-lines which may link any pair of nodes. The accuracy of the DLO result is therefore a function of the nodal density employed. Each model was evaluated using nodal spacings on a square grid of B/20, B/40 and B/80, which demonstrated convergence with 1% difference between the latter two results. The analyses reported in this paper were thus undertaken with a nodal spacing of B/40 and with the boundaries located at a sufficient distance so as not to constrain the identified failure mechanism. The commercial DLO code LimitState:GEO (LimitState, 2013) was employed in this study using a 1-dimensional 'engineered element' (which can undergo a plastic yielding in bending) to model the foundation. A no-tension condition was modelled on the soil/foundation interface.

The limit load evaluated from the EPFEM analyses is assumed to coincide with the load at which the convergence of the interactive procedure fails, provided the load-displacement curve of the foundation shows a horizontal plateau, denoting the formation of a rupture mechanism. Since it is well known that EPFEM method is not reliable for capturing limit state conditions, two commercial finite element codes have been employed: ABAQUS and PLAXIS, in order to evaluate the consistency of the numerical results with different meshes and boundary conditions. Figure 1 shows the typical finite element meshes used in the two

codes: about 8500 8-noded, parabolic elements were employed in ABAQUS (implying nearly 26000 nodes and 52000 unknowns), whereas 15 noded-triangular elements were used in PLAXIS. Uniform meshes were preferred with respect to optimised meshes (with smaller elements close to foundations), for an easier analysis of the effects of mesh size. Models with different nodal spacings on a square grid of B/10, B/20 and B/40, were employed in ABAQUS for load case A, in order to evaluate the accuracy of failure load versus mesh refinement: the numerical results show 0.05 % difference between the former two meshes and a much smaller difference between the latter two. The horizontal displacements were constrained on the lateral, vertical boundaries, whereas all displacements at the bottom were constrained in PLAXIS and only the vertical displacements in ABAQUS. The slight difference of the boundary condition at the bottom of the mesh was introduced to evaluate the variation of the numerical results. It will be shown below that the failure loads obtained with the different commercial codes are perfectly consistent with each other, because the lower boundary is sufficiently deep.

A no-tension kind of soil-foundation interface with null tangential stresses was considered with both ABAQUS and PLAXIS.

The typical computed response of applied load (expressed in terms of load multiplier) versus the vertical settlement of the foundation (in this case load case C and M_p = 200 kNm/m were considered) is shown in Fig. 2. Most analyses have been performed with ABAQUS, whereas the PLAXIS analyses were mostly undertaken for the purposes of verification.

Since FEM analyses apparently fulfil both equilibrium conditions and rupture criteria, they could be considered at a first glance to provide a lower bound solution. However the equilibrium condition is not exactly satisfied in FEM analyses (it is satisfied only in weak

form for a stress distribution which is not continuous at inter element boundaries), thus the limit loads computed with the FEM method cannot be consider a rigorous lower bound.

The limit load evaluated using the linear elastic (LW) and elasto-plastic Winkler model (NLW)

The limit load and maximum bending moments were tentatively evaluated also with a Winkler model incorporating linear elastic or linear elastic-perfectly plastic springs (that will be denoted below as elasto-plastic Winkler model) in order to determine to what extent a standard and enhanced Winkler model can capture the combined rupture mechanisms predicted by the more accurate methods discussed above. The elastic stiffness of the non-linear springs was assumed to equate to 3.555×10^6 kN/m^3 (corresponding to the stiffness value yielding the same mean settlement of a very long foundation lying on an elastic soil layer with E_u=20 MPa and Poisson ratio 0.5); for the elasto-plastic model, the limiting value of soil pressure is assumed to equate to q_{lim}=102.8 kPa (from the theoretical value of the limiting pressure of the shallow foundation per unit width). A no-tension kind of contact at soil-structure interface was modelled so that the foundation can detach from the subsoil.

Comparison between DLO and EPFEM analyses at ULS

Figs. 3(a), 3(c), 3(e) and 4(a), 4(c) and 4(e) show the deformed collapse slip line mechanisms evaluated with DLO code for the load cases A through C, in the cases of very large and very small resisting moments of the foundation. Figures 3(b), 3(d), 3(f) and 4(b), 4(d) and 4(f) show the deformed central portion of the FEM meshes (used with ABAQUS) and the contours of equivalent plastic strain amplitude for the load cases A through C, for very large and very small resisting moments M_p of the foundation and for different concrete section heights (h=31 cm and h=90 cm). It can be seen that there is a good qualitative match to the identified mechanisms.

When large resisting moments are considered, no plastic hinge forms in the foundation and the computed limit load can be compared with well-known theoretical values. In contrast, when small resisting moments are considered, one or more plastic hinges form in the foundation and the theoretical traditional analyses are not always possible. In the latter case the occurrence of a combined rupture mechanism is considered to occur.

The computed results are summarised in Tables 2-4 for load cases A through C, respectively. From these analyses the following conclusions can be drawn:

- in the case of a large resisting moment (lines 2 and 3 of Table 2) the good consistency of the EPFEM results obtained with h = 90 and h = 31 cm shows that the computed limit load is insensitive to the elastic stiffness of the foundation, as expected from plasticity theory;

- when no plastic hinge forms (first three-four lines of each Table), the limit load calculated with EPFEM and DLO is fairly consistent with conventional analysis;

- the lower the resisting moment of the foundation, the lower the limit load is, due to a combined rupture mechanism in the soil and in the foundation;
- in the case of a combined rupture mechanism, the evaluations obtained with different FEM codes (i.e. ABAQUS and PLAXIS) and DLO are consistent with each other to within a small margin.

Finally Fig. 5 shows the comparison between the bending moments calculated with the DLO and EPFEM analyses. Only load cases B and C, with M_p=200 kNm/m and M_p=500 kNm/m (Figs. 3(e), 3(f) and 4(c), 4(d), respectively) are considered for the sake of brevity. As illustrated by this case the comparison between the different numerical approaches is excellent.

The maximum bending moments evaluated with linear elastic Winkler (LW) and elasto-plastic Winkler (NLW) model

Load cases A and C were modelled using a linear elastic-perfectly-plastic springs, Winker (NLW) approach. The results in Tables 2 and 4 show that reasonably good results can be obtained with the NLW model, even in terms of foundation detachment. However the main drawback of the NLW model is that a reliable estimate of the limit value of soil pressure can be easily obtained only when the limit value of contact pressure is not very sensitive to the geometry of the portion of the foundation that is in contact with subsoil. Under undrained conditions this holds reasonably true because the influence of the shape factors on the limit value of contact pressure is fairly small, in contrast for a 2D slab foundation lying on

granular soil (or on clay under drained conditions) the evaluation of the limit value of subsoil pressure is made more difficult by the further dependence of the limit load on the width of the portion of foundation which is in contact with subsoil.

The bending moments at ULS loadings computed with the linear elastic Winkler (LW) model are significantly smaller (particularly for the low stiffness foundation) than the bending moments computed with the EPFEM/DLO computation and with the NLW model. This is fairly reasonable because the LW model cannot account for plastic contact pressure redistribution beneath the base of the foundation, thus the contact pressure can be locally much larger that the limiting value at rupture, and therefore does not require the foundation to spread the load laterally to other parts of the soil body to take the load. This consequently reduces the required bending moments. This is particularly evident for stiff foundations in which EPFEM analyses tend to produce a Boussinesq like pressure distribution with maximum pressure at the foundation edges, thus generating larger bending moments for a given load than LW model (that tends to produce a uniform pressure distribution).

Yield surface

The analyses presented in the previous Sections show that the ULS loads evaluated with the computational upper bound limit analysis (DLO procedure) and with the EPFEM analysis (both ABAQUS and PLAXIS FEM programs) are very consistent with each other, both in the

case of a rupture occurring only in the soil and, most importantly, in the case of a combined rupture mechanism.

Figure 6 shows the ultimate load versus the plastic bending moment, as evaluated with DLO and EPFEM procedures, in load cases A through C. These curves will be referred below with the term *ULS curves*. It can be observed that each curve has an initial curved part followed by a horizontal line: the curved part models the combined rupture mechanism, whereas the straight part concerns the rupture occurring only in the subsoil. Note that the *ULS curves* do not begin from the axis origin: for zero plastic bending moment, the ultimate load coincides with that of a fully flexible foundation.

For the sake of comparison, Figure 6 shows in addition the plot of maximum bending moments versus the applied load, resulting from soil-foundation interaction analysis and computed with different approaches, namely the EPFEM analysis, the linear Winkler model (LW) and the non-linear Winkler model (NLW). These curves will be referred below with the term *SLS curves*. The soil-foundation interaction analyses at SLS were performed under the assumption that the resisting plastic moment of the foundation is very large. A properly dimensioned beam must be represented in Fig. 6 by a point on the *SLS curve* lying entirely below the *ULS curves*. The *ULS curves* represent an upper bound limit, or type of yield surface, that gives the largest load that can be sustained for a given moment of resistance. The actual acceptable SLS loading will depend on the settlement criteria which is beyond the scope of this paper.

The *scaled-ULS curve* is also plotted and appears as a straight line in Fig. 6 joining the origin to the horizontal line representing the conventional ULS capacity. Since it has been established that the scaled-ULS analysis is a lower bound, then for a given maximum

bending moment, it will always predict a lower allowable maximum load when compared to the ULS maximum moment evaluated from a combined rupture mechanism (assuming that this is close to the true plastic solution). Alternatively the corollary is that for a given limit load, the maximum bending moment evaluated with the scaled-ULS is always larger than the ULS maximum moment evaluated from a combined rupture mechanism, thus a foundation structure which is dimensioned to resist a maximum bending moment derived from a scaled-ULS analysis would be safe though may lead to a large oversize of the foundation section for a given limit load.

The required bending moment from the scaled-ULS (conventional) analysis is typically larger than the FE based SLS but this is not universally true as shown by the EPFEM (h = 90 cm) results in case A. For a centrally loaded stiff foundation on an elasto-plastic undrained soil the pressure distribution will tend to produce a Boussinesq-like distribution with maximum pressures at the foundation edges and small pressure at foundation centre (in the form of an inverted parabola) leading to larger peak bending moment in comparison to an assumption of uniform pressures over the full length of the foundation. (Since this, and indeed any SLS solution is an equilibrium stress field nowhere violating yield it can simply be regarded as a generally poorer ULS lower bound than the scaled-ULS result).

Finally it is observed that the NLW approach does not always provide a good match with EPFEM for SLS loading. However NLW is conservative for determining the required ULS bending moment for a given load. As expected this is not true for LW which is always inappropriate for ULS analysis and appears to match the NLW analysis only for loads approximately less than half the ULS load based on the cases studied. (It is also noted that the EPFEM analysis for h = 31 cm does exceed the ULS curve by a small amount. However

this is attributed to numerical tolerances. It would be expected that the curves simply merge).

Discussion

A shallow foundation of the type investigated should be sized to satisfy SLS and ULS considerations. In terms of bending strength, the designer may choose a strength, M_p, based on a simple ULS soil rupture only analysis (the start of the straight, horizontal, line portion of the ULS curves in Fig. 6). This will definitely suffice to avoid ULS but is likely to be very overconservative value of the bending strength M_p at lower loads.

In contrast an economic ULS design should be based on combined rupture analysis given by the curved portion of the ULS curves in Fig. 6. As would be expected, and examining Fig. 6, the ULS load capacity for a given bending strength M_p is always larger than the computed SLS load corresponding to a maximum bending moment $M_{max} = M_p$. An SLS load/moment combination is a valid stress distribution in equilibrium and nowhere violating yield (if $M_p = M_{max}$). Using the lower bound theorem the SLS load will always be carried but a larger or equal load may be carried before reaching ULS. This will be true of SLS results generated using EPFEM results (though this may not be fully rigorous if the FEM analysis satisfies equilibrium in a weak form only). It is interesting to note that the results generated by NLW in the current study also seem to generate consistent lower bounds, but this is not proven in general.

While it follows that, for a given load, the given required bending strength from the graph is always less than the SLS maximum bending moments, it must be remembered that a ULS

design calculation will typically be subjected to much larger factors of safety than a SLS design calculation and this will mean that SLS governs in some cases while ULS will govern in others. The choice of factoring approaches therefore also may have a significant influence on the design. This is an area that requires further investigation.

CONCLUSIONS

This work explores for the first time (to the best of the authors' knowledge) how the limit load of a shallow foundation is affected by the occurrence of a combined rupture mechanism involving both the soil and the foundation. This analysis is performed by using two different numerical approaches (namely DLO and EPFEM analyses) for a simple 2D problem under undrained conditions. The excellent consistency among the different numerical results support the reliability of the numerical evaluations, for which neither analytical nor experimental evaluation has been proposed so far.

The main conclusions can be summarised as follows.

1. Both ULS DLO and EPFEM analyses provide an upper load limit, expressed in terms of ultimate load vs resisting moment, which can never be passed by the maximum bending moment vs applied load relationships evaluated at working SLS state (by using EPFEM methods). This upper limit represents the locus of the conditions in which the strength of all materials in the system (namely both the soil and the foundation) is fully mobilized (namely the so-called combined rupture mechanism). This can be regarded as a yield or limit surface for the soil-foundation system.

2. A design based on a moment resistance calculated from a simple soil rupture only ULS analysis (with foundation assumed rigid) should always be safe (lower bound). For undrained problems, the limit soil pressure can be assumed constant along the effective bearing width, although this assumption might lead to unexpectedly large, moment resistances in the case of flexible foundations.

3. Simple parallel scaling down of ULS loads and moments (scaled-ULS) from such an analysis can also be shown to give a lower bound. In other words, such an analysis will give conservative overestimates of the required ULS foundation bending strength (or equivalently an underestimate of the ULS load for a given bending strength) for undrained problems.

4. If soil pressures are kept below the limiting value by using an elasto-plastic Winkler model (thus at no point the predicted soil pressure exceeds the plastic limit bearing value), then reasonable estimates of SLS design moments can be obtained comparable to EPFEM methods, especially for low stiffness foundations. However the plastic limit bearing pressure can only be explicitly defined for undrained conditions and for a 2D problem or a foundation beam, because in the other cases (under a foundation slab in 3D conditions or for drained loads) the plastic limit bearing pressure depends on the effective dimensions of the foundations (thus an implicit calculation is necessary).

5. Caution must be used with elastic Winkler models. Particularly for low-stiffness foundations, maximum predicted bending moments may strongly underestimate those required to avoid a ULS condition.

6. A combined rupture ULS analysis should lead to more efficient foundation design. However both SLS and ULS conditions must be considered and their interplay will be a function of the nature of the safety factoring adopted.

At present, there is the need of practical and an expeditious means of analysis of combined rupture mechanisms for beams and slabs, under both undrained and drained conditions, that could be easily and generally employed in practical design analysis (i.e. something similar to Broms' method for flexible piles subjected to horizontal loading).

Acknowledgments

The financial support from the European Union ERC advanced grant 'Instabilities and nonlocal multiscale modelling of materials' ERC-2013-AdG-340561-INSTABILITIES (2014–2019) is gratefully acknowledged by A. Gajo.

REFERENCES

1 Brinkgreve, R.B.J. (2002). Plaxis 2D- Version 8. Balkema, Lisse.

2 Burland, J., Chapman, T., Skinner, H. & Brown, M. (2012). ICE Manual of geotechnical engineering.
3 ICE Publishing, London.

4 Chen, W.F. (2007). Limit Analysis and Soil Plasticity, J Ross Publishing.

5 Duncan, J.M. & Buchigani, A.L. (1976). An engineering manual for settlement studies. Dept.
6 of C.E., University of California, Berkley.

7 Hibbitt, Karlsson & Sorensen (2009). ABAQUS/Standard User's Manual, Version 6.9. *Hibbitt, Karlsson*
8 *& Sorensen, Inc.*, Pawtucket, R.I.

9 LimitState (2013), LimitState:GEO Manual VERSION 3.1b, October 2013 edn, LimitState Ltd.

10 Fang, H.Y. (1991). Foundation engineering handbook. Van Nostrand Reinhold, New York.

11 Frank R., Baudin, C., Driscoll, R., Kavvadas, M., Krebs Ovesen, N., Orr, T. & Schupper, B. (2004).
12 Designers' guide to EN 1997-1. Tomas Telford Publishing, London.

13 EN 1997-1 (2004). Eurocode 7: Geotechnical design - Part 1: General rules [Authority: The European
14 Union Per Regulation 305/2011, Directive 98/34/EC, Directive 2004/18/EC].

15 Meyerhof, G.G. (1953). The bearing capacity of foundations under eccentric and inclined loads.
16 Proc., 3rd Int. Conf. on Soil Mech. And Found. Engrg., 1,440-445.

17 Smith, C.C. & Gajo, A. (2015) Combined rupture mechanisms in shallow foundations. Part II
18 Implications for Eurocode 7 Assessment. In submission.

19 Smith, C.C. & Gilbert, M. (2007). Application of discontinuity layout optimization to plane plasticity
20 problems. Proceedings of the Royal Society A: Mathematical, Physical and Engineering Sciences, 463
21 (2086), October, pp 2461-2484. ISSN 1364-5021.

Smoltczyk, U. (2003), Geotechnical engineering handbook. Ernst & Sohn, Berlin.

Ukritchon, B., Whittle, A.J. & Sloan, S.W. (1998). Undrained limit analysis for combined loading of strip footings on clay. J. Geotech. Geoenviron. Engng, ASCE 124, No. 3, 265–276.

Ukritchon, B., Whittle, A.J. & Sloan, S.W. (2003). Undrained stability of braced excavations in clay. ASCE Journal of Geotechnical and Geoenvironmental Engineering, 129(8), 738-756.

Vardanega, P. J. & Bolton, M. D (2011). Strength mobilization in clays and silts. Can. Geot. J., 48, 10, 1485-1503.

List of symbols

B	width of foundation
B’	reduced width of foundation
c_u	undrained shear strength
d	embedment depth
E_u	undrained elastic modulus

1	E	elastic modulus of concrete
2	EJ	foundation bending stiffness
3	f_{bk}	characteristics concrete strength
4	h	height of foundation section
5	M	bending moment
6	M_{max}	maximum bending moment
7	M_p	bending strength
8	N_{lim}	limit load
9	N_c, N_q, N_γ	bearing capacity factors
10	m, n	scale factors
11	q	surcharge pressure at the foundation base
12	q_{lim}	limit pressure beneath the foundation
13	x	horizontal distance from the centre of the foundation
14	γ	unit weight of soil
15		
16		
17		
18		

List of figure captions

Figure 1. Finite element mesh employed with (a) ABAQUS and (b) PLAXIS FEM codes.

Figure 2. Typical load displacement curve computed for load case (c) with ABAQUS: h=31cm and M_p=200 kNm/m.

Figure 3. Load case A: M_p = 500 kNm/m, with plastic hinge at x = 0.00 m: (a) CLA solution, (b) FEM solution (h=31 cm); load case A: M_p = 1200 kNm/m: (c) CLA solution, maximum bending moment 1032kNm/m, (d) FEM solution, maximum bending moment 1073kNm/m and h=90 cm; load case B: M_p = 200 kNm/m, with plastic deformation from -1.80 m to +1.80 m: (e) CLA solution, (f) FEM solution (h=31 cm).

Figure 4. Load case B: M_p = 800 kNm/m (a) CLA solution, max bending moment at foundation centre is 770 kNm/m, (b) FEM solution, max bending moment at foundation centre is 760 kNm/m and h = 90cm; load case C:, M_p = 200 kNm/m: (c) CLA solution, with plastic hinge at *x* = 1.75 m, (d) FEM solution (h=31 cm), with plastic hinge at *x* = 1.50 m; load case C: M_p = 500 kNm/m: (e) CLA solution, max bending moment 465 kNm/m, (f) FEM solution, max bending moment 466 kNm/m and h = 90 cm.

Figure 5. Bending moment distribution computed with DLO and EPFEM analyses for h = 31 cm. (a) load case B and M_p=200 kNm/m. (b) load case C and M_p=500 kNm/m.

Figure 6. Ultimate load vs resisting moment (for DLO and EPFEM analyses) and maximum bending moment vs applied load for soil-foundation interaction analyses (EPFEM, NLW and LW), evaluated for very large beam resisting moments: load cases A, B and C.

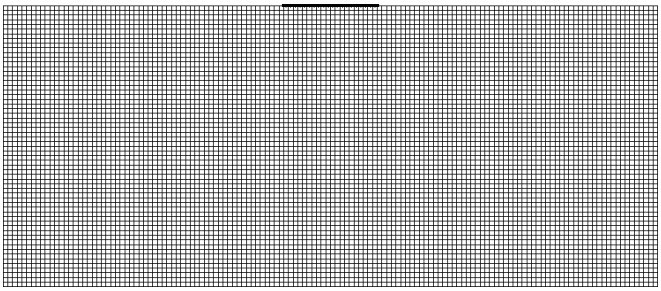

a)

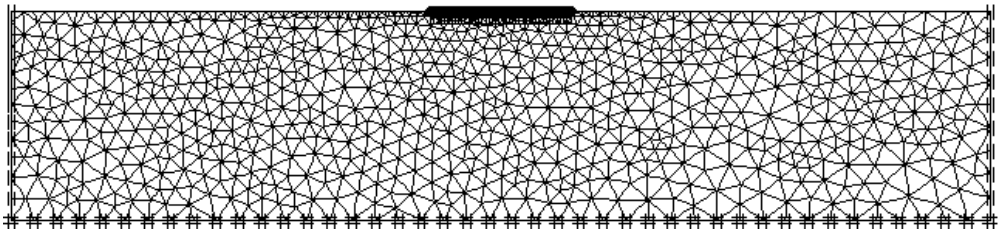

b)

Figure 1. Finite element mesh employed with (a) ABAQUS and (b) PLAXIS FEM codes.

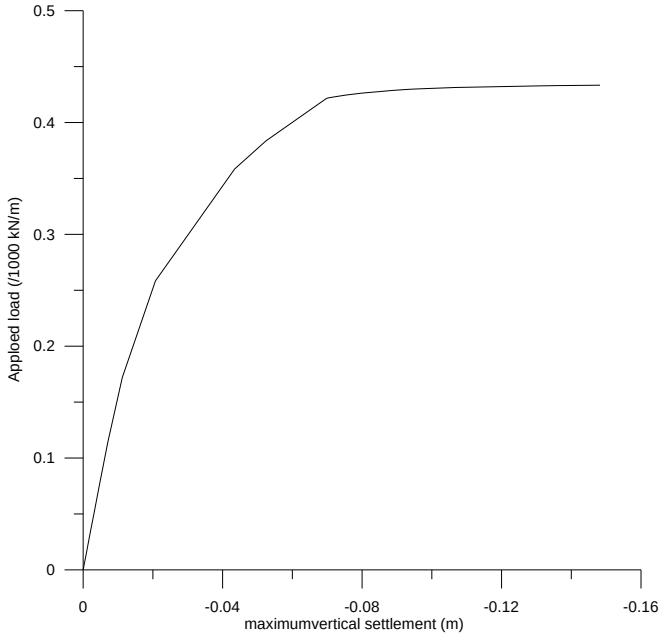

Figure 2. Typical load displacement curve computed for load case (c) with ABAQUS: h=31cm and M_p=200 kNm/m.

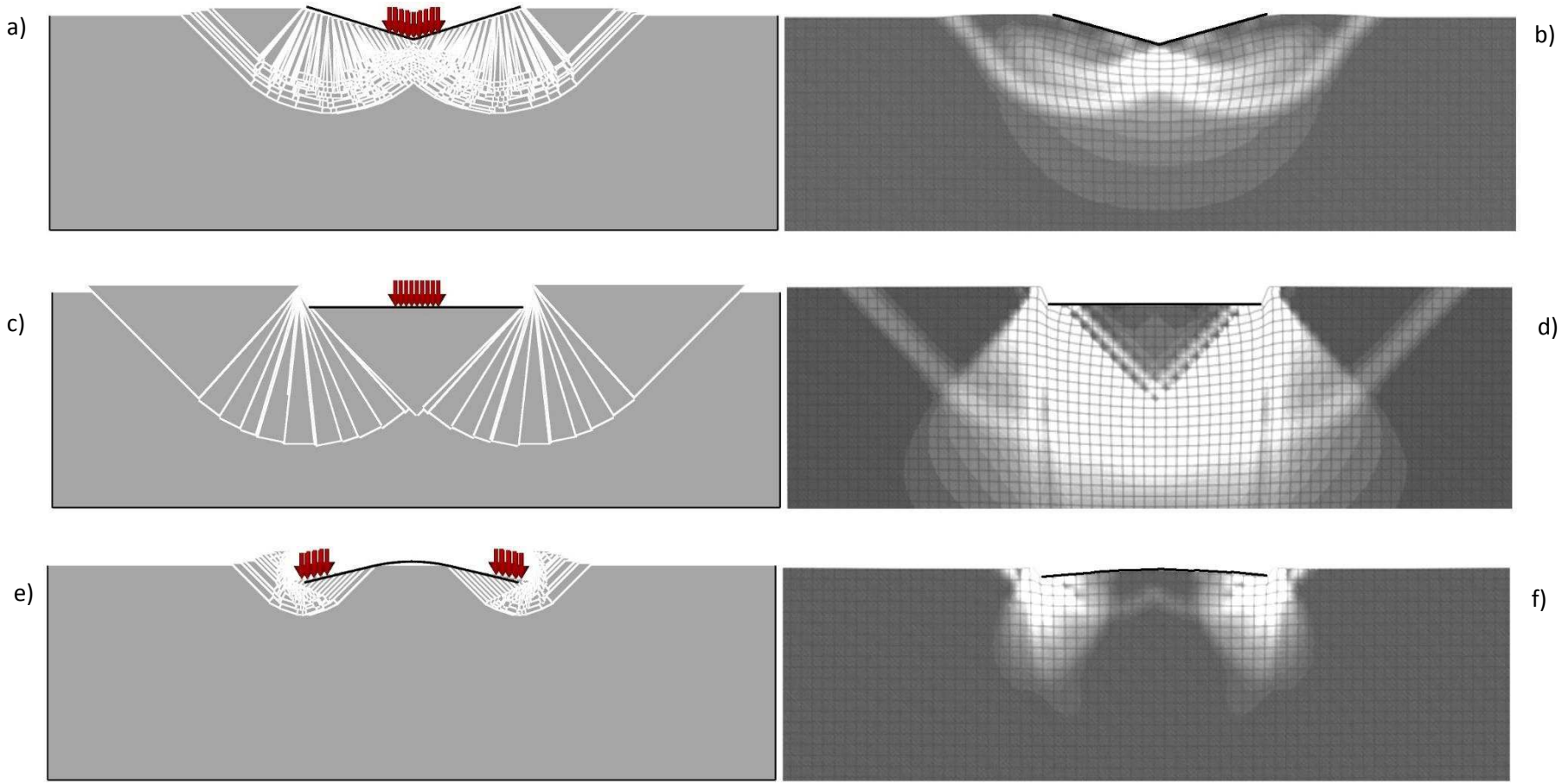

Figure 3. Load case A: M_p = 500 kNm/m, with plastic hinge at x = 0.00 m: (a) CLA solution, (b) FEM solution (h=31 cm); load case A: M_p = 1200 kNm/m: (c) CLA solution, maximum bending moment 1032kNm/m, (d) FEM solution, maximum bending moment 1073kNm/m and h=90 cm; load case B: M_p = 200 kNm/m, with plastic deformation from -1.80 m to +1.80 m: (e) CLA solution, (f) FEM solution (h=31 cm).

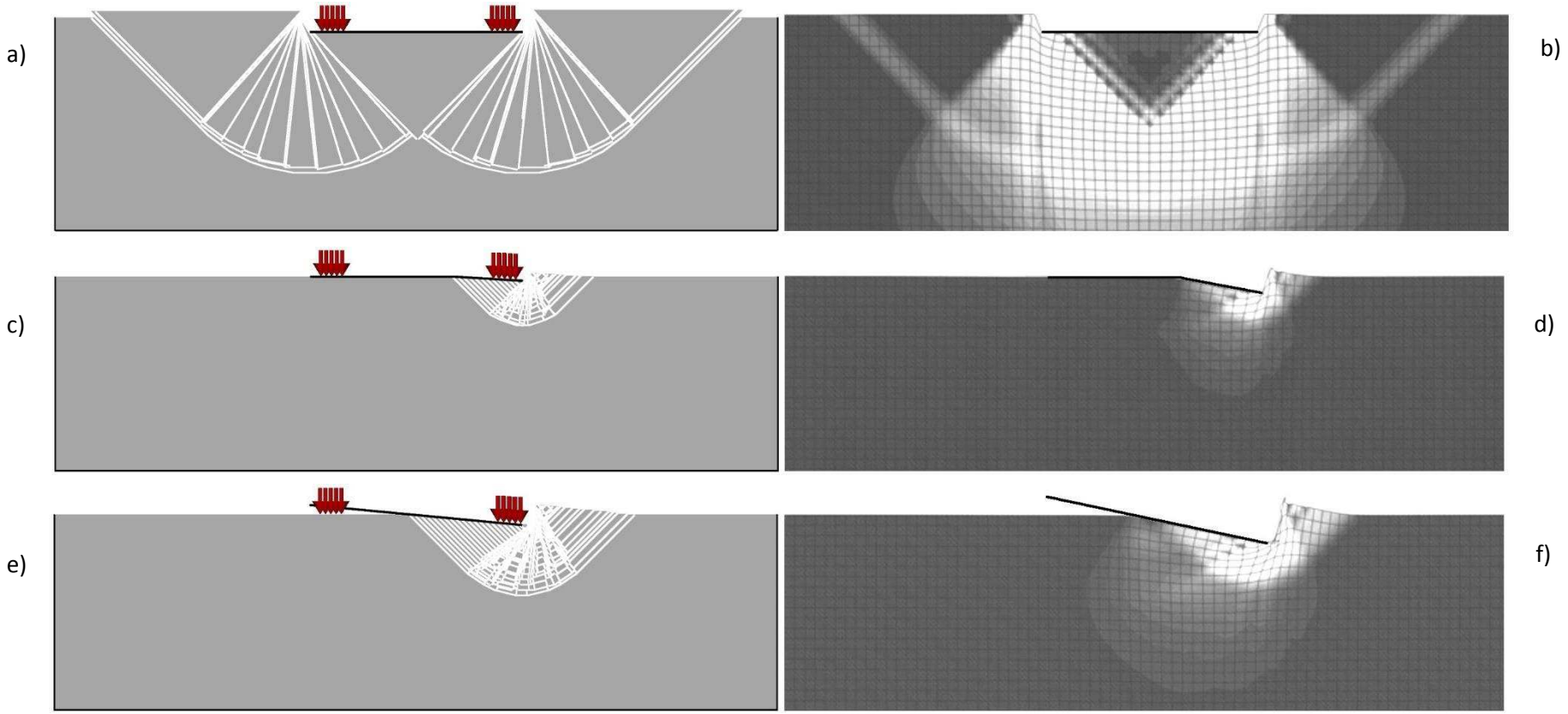

Figure 4. Load case B: M_p = 800 kNm/m (a) CLA solution, max bending moment at foundation centre is 770 kNm/m, (b) FEM solution, max bending moment at foundation centre is 760 kNm/m and h = 90cm; load case C:, M_p = 200 kNm/m: (c) CLA solution, with plastic hinge at *x* = 1.75 m, (d) FEM solution (h=31 cm), with plastic hinge at *x* = 1.50 m; load case C: M_p = 500 kNm/m: (e) CLA solution, max bending moment 465 kNm/m, (f) FEM solution, max bending moment 466 kNm/m and h = 90 cm.

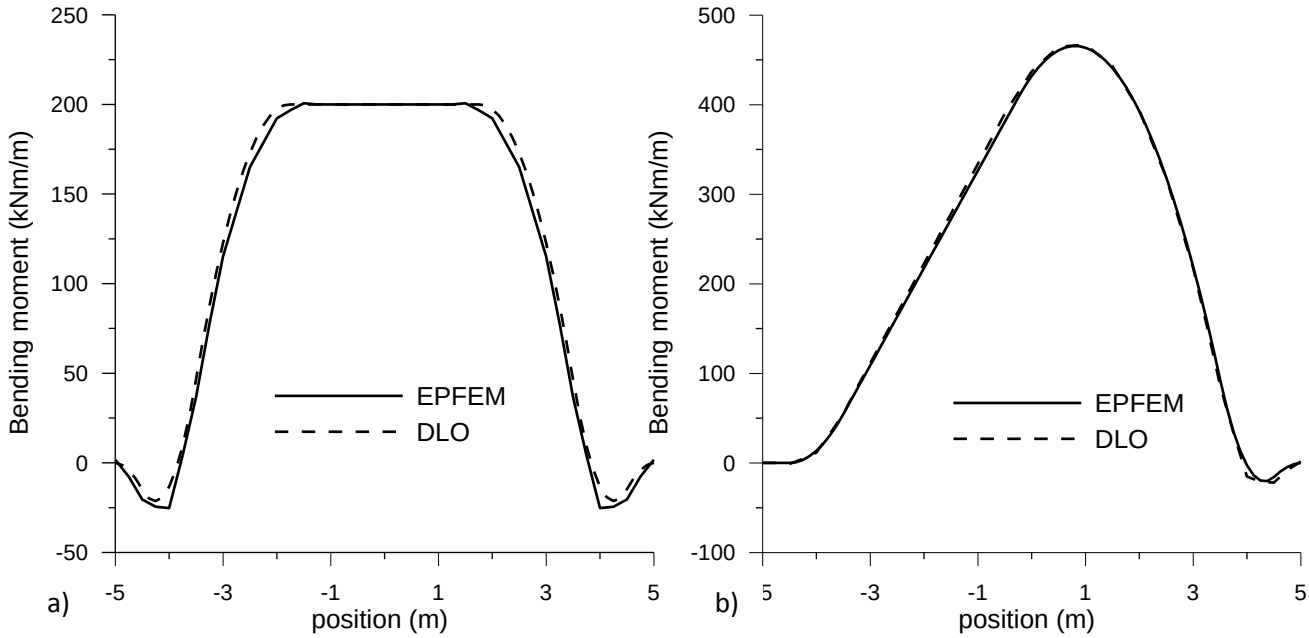

Figure 5. Bending moment distribution computed with DLO and EPFEM analyses for h = 31 cm. (a) load case B and M_p=200 kNm/m. (b) load case C and M_p=500 kNm/m.

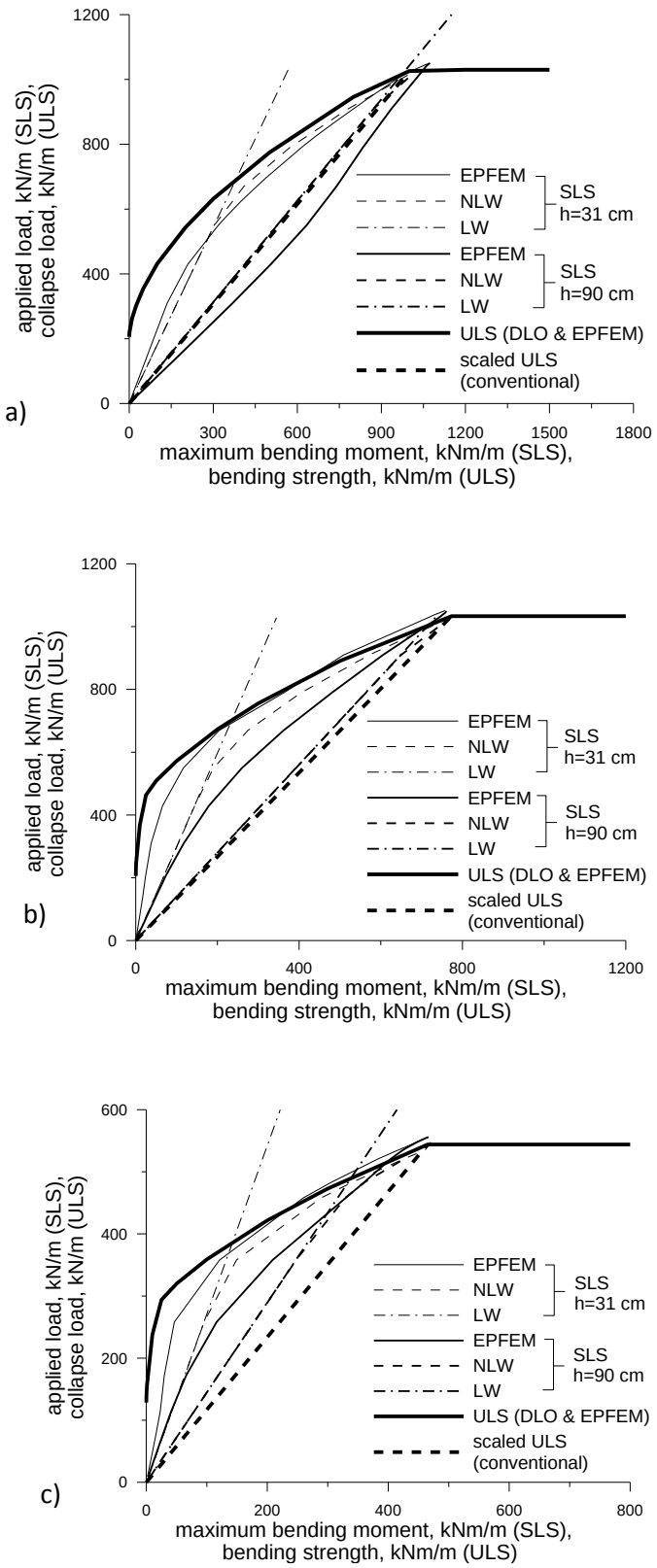

Figure 6. Ultimate load vs resisting moment (for DLO and EPFEM analyses) and maximum bending moment vs applied load for soil-foundation interaction analyses (EPFEM, NLW and LW), evaluated for very large beam resisting moments: load cases A, B and C.

A: central loading	B: split symmetrical loading	C: split asymmetrical loading
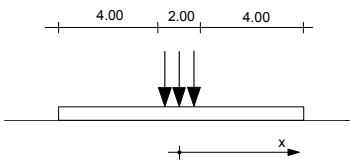	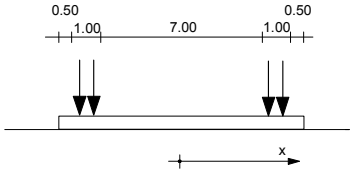	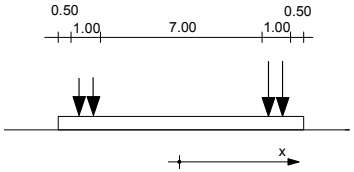
c_u=20 kPa q_{lim}= (2+π) c_u=102.8 kPa		
e = 0 B' = 10 m	e = 0 B' = 10 m	e = 2.40 m B' = 5.20 m
N_{lim} = 10.00 x 102.8 = 1028 kN/m	N_{lim} = 10.00 x 102.8 = 1028 kN/m	N_{lim} = 5.20 x 102.8 = 535 kN/m
N_{lim}^* = 1028 kN/m		
N_{lim} / N_{lim}^* = 1	N_{lim} / N_{lim}^* = 1	N_{lim} / N_{lim}^* = 0.52
M_{max} = 2.50 x N_{lim} /2 – 0.50 x N_{lim} /2 = 1.00 x N_{lim} = 1028 kNm/m	M_{max} = 2.50 x N_{lim} /2 – 4.00 x N_{lim} /2 = -0.75 x N_{lim} = -771 kNm/m	M_{max} = 0.5 x (5.00-0.84) ^{2} x N_{lim} /5.20 – (4.00-0.84) x 0.80 x N_{lim} = -0.864 x N_{lim} = -462 kNm/m
$M_{max}/q_{lim}B^2$ = 1x10^{-3}	$M_{max}/q_{lim}B^2$ = -0.75x10^{-3}	$M_{max}/q_{lim}B^2$ = -0.45x10^{-3}

Table 1. Schematics of the load cases and principal relationships. *B'* is the effective bearing width of the foundation

Resisting moment (kNm/m)	Concrete section height (m)	Analysis method	Limit load (kN/m)	M_{max} (kNm/m) or plastic hinge location
Rigid		CONVENTIONAL	1028	1028
1200	0.90	EPFEM (ABAQUS)	1050	1074
	0.31	EPFEM (ABAQUS)	1050	1073
	-	DLO	1030	1032
1000	-	DLO	1026	one at x=0.00 m
	0.31	NLW (ABAQUS)	1021	one at x=0.00 m
800	0.90	EPFEM (ABAQUS)	935	one at x=0.00 m
	0.90	EPFEM (PLAXIS)	946	one at x=0.00 m
	-	DLO	945	one at x=0.00 m
	0.90	NLW (ABAQUS)	923	one at x=0.00 m
500	0.31	EPFEM (ABAQUS)	764	one at x=0.00 m
	0.31	EPFEM (PLAXIS)	763	one at x=0.00 m
	-	DLO	774 (790)	one at x=0.00 m
N/A	0.90	LW (ABAQUS)	1028	985
	0.31	LW (ABAQUS)	1028	566

Table 2. Parameters evaluated for load case A, with x the distance of plastic hinge from the centre of the foundation. The computed conventional limit load was used as the applied load in the LW analysis.

Resisting moment (kNm/m)	Concrete section height (m)	Analysis method	Limit load (kN/m)	M_{max} (kNm/m) or plastic hinge location
Rigid	-	CONVENTIONAL	1028	771
800	0.90	EPFEM (ABAQUS)	1050	760
	-	DLO	1033	770
500	0.31	EPFEM (ABAQUS)	907	465
	0.31	EPFEM (PLAXIS)	915	475
	-	DLO	891 (896)	-0.6m to 0.6m
200	0.31	EPFEM (ABAQUS)	682	Continuous plastic bending between -1.8m and +1.8m
	0.31	EPFEM (PLAXIS)	676	M > 195 kNm/m between -0.70 and 0.70, M_{max} = 197 kNm/m
	-	DLO	667(680)	Continuous plastic bending between -1.8m and +1.8m
N/A	0.90	LW (ABAQUS)	1028	733
	0.31	LW (ABAQUS)	1028	345

Table 3. Parameters evaluated for load case B, with x the distance of plastic hinge from the centre of the foundation. The computed conventional limit load was used as the applied load in the LW analysis.

Resisting moment (kNm/m)	Concrete section height (m)	Analysis method	Limit load (kN/m)	M_{max} (kNm/m) or plastic hinge location
Rigid	-	CONVENTIONAL	535	462 at 0.84 m
500	0.90	EPFEM (ABAQUS)	556	466 at 1.00 m
	0.90	EPFEM (PLAXIS)	564	None
	-	DLO	544	465 at 0.88 m
	0.90	NLW (ABAQUS)	591	500
300	0.31	EPFEM (ABAQUS)	484	one at x=1.00 m
	-	DLO	473	one at x= 1.37 m
	0.31	NLW (ABAQUS)	466	one at x=1.50 m
200	0.31	EPFEM (ABAQUS)	433	one at x=1.50 m
	-	DLO	422	one at x= 1.75 m
100	0.31	EPFEM (ABAQUS)	371	one at x=2.00 m
	-	DLO	359	one at x =2.25m
N/A	0.90	LW (ABAQUS)	535	369
	0.31	LW (ABAQUS)	535	197

Table 4. Parameters evaluated for load case C, with x the distance of plastic hinge from the centre of the. The computed conventional limit load was used as the applied load in the LW analysis.